Evidence for significant radial increase of the mass-to-light ratio based on phenomenological analysis of eight early-type galaxies

Srdjan Samurović[1],
Astronomical Observatory, Volgina 7, 11060 Belgrade, Serbia
srdjan@aob.bg.ac.rs
(Submitted on 09.07.2015; Accepted on 20.07.2015)

Abstract. In this paper we study the sample of eight nearby early-type galaxies for which we have reliable estimates of their total dynamical mass in their interior and exterior parts based on the observed globular clusters. We use a phenomenological approach in the study of the gradient of the mass-to-light ratio of the galaxies in the sample. Since the outermost point for which we have the estimates of the mass-to-light ratios is fixed at 5 effective radii, this provides the opportunity to study the dark matter content of early-type galaxies which is expected to dominate in their outer parts, i.e., beyond $\sim 2-3$ effective radii. We find that all the galaxies in our sample show the increase of the cumulative mass-to-light ratio which indicates various amount of additional, dark, component in their mass content. We show that galaxies with higher values of $\alpha+\beta$ (where α and β are slope parameters) have higher virial masses. We show that two galaxies which are slow rotators (NGC 1407 and NGC 5846) have $\alpha+\beta>1$ whereas the remaining 6 galaxies are all fast rotators, and for these objects we found that $\alpha+\beta\leq 1$. We also compare our findings with the theoretical expectations coming from numerical simulations.

Key words: galaxies: kinematics and dynamics — galaxies: elliptical and lenticular — galaxies: structure – dark matter — galaxies: individual: NGC 1400, NGC 1407, NGC 2768, NGC 3115, NGC 3377, NGC 4278, NGC 4494, NGC 5846

Introduction

It is now well established that most of the galaxies in the Universe are found in dark matter halos. The case of late-type (spiral) galaxies is well studied and the widely accepted opinion is that they need significant amount of dark matter (DM) or modification of Newtonian gravity is necessary. On the other hand, the case of early-type (elliptical and lenticular) galaxies (hereafter ETGs) has been less studied, and the reasons for this situation are, for example, low surface brightness and lack of tracers of the total dynamical mass in their outer parts (see Samurović 2007a for details). In the recent years, however, new observational data has been collected that are relevant for the studies of the kinematics and dynamics of ETGs and this lead to the possibility of application of various already available theoretical concepts. For example, various observations of globular clusters (GCs) and planetary nebulae (PNe) are now available and can be used to infer the contribution of DM in ETGs. In the present paper we will use GCs as a tracer of total dynamical mass for a sample of 8 ETGs for which we analyze the mass profiles interior to 5 effective radii (R_e). The galaxies from our sample were analyzed in detail in Samurović (2014, hereafter S14) using the Jeans equation in both Newtonian and MOND (MOdified Newtonian Dynamics) approaches. The plan of the paper is as follows: in Section 1 we describe the theoretical approach used, in Section 2 we provide details about our sample of observed galaxies, in Section 3 we present our results and, finally, in Section 4 we summarize our findings and present the conclusions.

1. Theoretical considerations

In our analysis below we will rely on the phenomenological approach to modeling of ETGs: this is an intermediate approach between observations and theory and we applied it previously on ETGs in Samurović (2007b, hereafter S07b) and Samurović (2007c, hereafter S07c). Both of these papers were based on the work of Tortora, Cardona & Piedipalumbo (2007, hereafter TCP07) who suggested a double power law expression for the global cumulative mass-to-light (hereafter M/L) ratio of elliptical galaxies. Their ansatz can be written as:

$$\Upsilon(r) \equiv \frac{M(r)}{L(r)} = \Upsilon_0 \left(\frac{r}{r_0}\right)^{\alpha} \left(1 + \frac{r}{r_0}\right)^{\beta}, \tag{1}$$

where Υ_0 is a scaling M/L ratio, r_0 is a reference radius (in this paper taken to be R_e, i.e., effective radius which encompasses half the total light of a given galaxy) and (α, β) are slope parameters. The value of Υ_0 is based on the matter in the *inner* parts of the galaxies in our sample and is close to the value based on the stellar matter only because in the inner regions of ETGs the ordinary, stellar, component is dominant (see e.g., Samurović 2007a). The constant M/L ratio case is obtained for $(\alpha, \beta) = (0, 0)$ which leads to $\Upsilon(r) = \Upsilon_0$. TCP07 noted that a model without dark matter will thus be obtained by setting zero values for the two slope parameters: $\Upsilon(r) \simeq \Upsilon_*$, where Υ_* is then approximately equal to the value of the M/L ratio of the stellar component.

The constraints on the slope parameters are given as:

$$\max(\gamma - 2, -\beta) \leq \alpha \leq \min(\gamma, 1 - \beta), \tag{2}$$

and we refer the reader to TCP07 for more details. In this paper we use the Hernquist (1990) model of the luminosity density and thus $\gamma = 1$ is always used (see TCP07 for details). We vary the values of both α and β parameters within the limits provided in equation 2, but when the solution could not be found, we broaden the given range (see below for the case of NGC 5846).

We note here that we will fix the value of the M/L in the inner parts of of the galaxies of our sample to the value obtained using the Jeans modeling as given in S14.

In order to compare our results based on observations to theoretical predictions we will use Navarro, Frenk & White (NFW) (1996, 1997) models based on N-body simulations of hierarchical collapse and merging of cold dark matter (CDM) haloes which produce an universal density profile:

$$\rho_{\rm NFW}(r) = \frac{\rho_s}{(r/r_s)(1 + r/r_s)^2}, \tag{3}$$

where r_s is the inner characteristic length-scale, which corresponds to the radius where the logarithmic slope of the profile is equal to -2 and ρ_s is the density at that radius. One can define the concentration parameter

$c_{\rm vir} \equiv r_{\rm vir}/r_s$, where $r_{\rm vir}$ is the halo virial radius (see Bullock et al. 2001). As in S07c, we will compare the results based on the CDM theory according to which the halo concentration correlates well with the virial mass: low-mass haloes are denser and more concentrated than high-mass haloes. According to Wechsler et al. (2002) and their numerical experiments, at redshift $z = 0$ the following relation holds (see also Boriello et al. 2003):

$$c(M_{\rm vir}) \simeq c_{11} \left(\frac{M_{\rm vir}}{10^{11} M_\odot} \right)^{-0.13}, \qquad (4)$$

where $c_{11} \simeq 20.8$. One of the main results of Wechsler et al. is that virtually no haloes are found below $c_{\rm vir} \sim 10$. This limit is shown in our Figure 3 below, and the galaxies are distributed according to the estimates of their concentration parameters for both theoretical predictions and observationally established values.

2. Observational data

We use sample of ETGs from the SLUGGS (SAGES Legacy Unifying Globulars and Galaxies Survey) database[1] (Pota et al. 2013, hereafter P13). SLUGGS combines Subaru/Supreme-Cam wide-field imaging with spectra obtained using the Keck/DEep Imaging Multi Object Spectrograph (DEIMOS). This sample is based on high velocity resolution data and the galaxies span a wide range of luminosities, morphological types (within the early-type class) and come from different environments (NGC 3115 is a field galaxy and the remaining objects belong to various groups of galaxies). The basic observational data is given in Table 1. The reader is referred to P13 and S14 for more details regarding the observational features of each galaxy.

It is important to stress that in this paper we work on the sample of galaxies for which: i) the kinematics for all the objects was based on the same tracers, GCs, ii) the M/L ratios were established at the same galactocentric distances, at $1R_e$ and $5R_e$, iii) all the estimates of the M/L ratios were obtained using the same technique, the application of the Jeans equation and iv) the estimates of the M/L ratios for all the galaxies were obtained taking into account orbital anisotropies (see S14 for details).

We selected 8 galaxies from S14 for which we had the observational data out to 5 R_e and we thus excluded two galaxies analyzed in S14 (NGC 4365 and NGC 4486) for which the outermost analyzed radius is well below $5R_e$. Two of the galaxies from the present sample were analyzed in S07b and S07c: NGC 4494 and NGC 5846. The comparison with the previous results will be given below.

In this paper we use the value of the Hubble constant $h_0 = 0.70$. All the values of the M/L ratios are expressed in the B-band.

[1] `http://sluggs.swin.edu.au`

Table 1. Basic observational data of the galaxies in the sample.

name	distance [Mpc]	1 arcsec [pc]	M_B	morpholog. type	environ.	R_e [arcsec]	profile	rotator
(1)	(2)	(3)	(4)	(5)	(6)	(7)	(8)	(9)
NGC 1400	26.8	129.98	−20.35	S0/E0	G	31	0	f
NGC 1407	26.8	129.98	−21.49	E0	G	72	0	s
NGC 2768	21.8	105.73	−21.26	E6/S0$_{1/2}$	G	93	D	f
NGC 3115	9.4	45.59	−19.94	S0	F	85	D	f
NGC 3377	10.9	52.87	−19.32	E6	G	46	D	f
NGC 4278	15.6	75.66	−19.50	E1-2	G	34	B	f
NGC 4494	16.6	80.51	−21.07	E1-E2	G	53	D	f
NGC 5846	24.2	117.37	−21.34	E0	G	61	B	s

NOTES – Column (1): name of the galaxy. Column (2): distances to the galaxies in the sample. Column (3): 1 arcsec expressed in parsecs. Column (4): B-band absolute magnitude. Column (5): morphological type. Column (6): environment of each galaxy ("G" means that the galaxy belongs to a group and "F" is a field galaxy). Column (7): value of the effective radius. Column (8): mean isotope shape ("D" indicates disky isophotes, "B" indicates boxy isophotes and "0" indicates pure ellipses). Column (9): central rotator type ("s" indicates slow and "f" indicates fast rotators). The references for the values found in Columns (2) – (9) are given in S14.

3. Computational results

In our calculations of the slope parameters α and β, we relied on our FORTRAN code which varies the slope parameters and fits equation 1 to the observed values of the mass-to-light ratio of a given galaxy. We have calculated the $\bar{\chi}^2$ values in each case and present the results in Figures 1 and 2 as well as in Table 2.

As in S07b, the following procedure was used: first, for each galaxy we tabulated 20 "observational" (i.e. based on the two observed values of the mass-to-light ratio at $1R_e$ and $5R_e$ assuming a linear relation between them) equidistant points which describe the mass-to-light ratio as a function of radius. Then, we vary the slope parameters while keeping the scaling mass-to-light ratio (Υ_0) constant and equal to the values established in the inner part of each galaxy as found in S14. In Figures 1 and 2 and in Table 2 we present the best-fitting results. In Figure 1 we plotted with the solid lines the observed mass-to-light ratios and with the dashed lines upper and lower limits of the fitted values of the mass-to-light ratios. These limits are inferred using various assumptions on radial anisotropies, as described in S14.

We found for all the galaxies in our sample: $\alpha + \beta > 0$. There is no galaxy for which $\alpha + \beta = 0$, or $\alpha = 0$ and $\beta = 0$, and thus no galaxy can be described without the inclusion of DM. The galaxies with higher values of $\alpha + \beta$ have also higher values of their virial mass (see the example of NGC 5846).

The fit obtained using the values (α, β) presented in Table 2 is between the two limits given with the dashed lines in Figure 1. From the positions of the galaxies in the (α, β) space given in Figure 2 one can see that only for one galaxy, NGC 5846, the position of the (α, β) pair is inconsistent with the predictions from equation 2. The estimate for NGC 1407 is marginally consistent with the predictions. Both of these galaxies have large virial masses, the largest among all the objects in our sample: NGC 1407 has the largest virial mass in the sample and is followed by NGC 5846.

In Figure 3 one can see that for 3 galaxies the theoretical predictions of the concentration parameter based on numerical simulations (see equation 4 and Table 3[2] are relatively close to the observationally inferred values of the same parameter and found above $c_{\rm vir} = 10$ for the following objects: NGC 4278 (best agreement), NGC 3115 and NGC 5846. For the remaining 5 objects the discrepancies are huge (except for NGC 1407) and the observational values are below the theoretical limit given by $c_{\rm vir} = 10$. The following result is obvious: the 3 galaxies for which $\alpha + \beta < 0.50$ all show huge discrepancies of the inferred value of the concentration parameter. We also refer the reader to Figure 24 of S14 where the relation between the concentration parameter and virial mass is presented: only one galaxy (NGC 1407) was found to be within the range of values expected from the ΛCDM model.

When inspecting Figure 3 further one can reach the following interesting conclusion: the two galaxies which are *slow* rotators (NGC 1407 and NGC 5846) have $\alpha + \beta > 1$ whereas the remaining 6 galaxies are all *fast* rotators and for these objects the following relation holds: $\alpha + \beta \leq 1$ (see Table 2 and Figure 3).

The galaxies with lower virial masses ($M_{\rm vir} < 1.1 \times 10^{12} M_\odot$) have lower values of $\alpha+\beta$: the galaxies NGC 1400, NGC 2768, NGC 3377 and NGC 4278 all have $\alpha + \beta \leq 0.50$. The galaxies with higher values of the virial mass ($M_{\rm vir} > 1.1 \times 10^{12} M_\odot$) all have $\alpha + \beta > 0.50$.

Two of the galaxies studied in the present paper were also analyzed previously using the same methodology: NGC 4494 (in S07b,c) and NGC 5846 (S07c). Since in the present work we used the updated and more accurate data, some differences were inevitable and they are as follows:

a) for the galaxy NGC 4494 the following pair was previously inferred (see S07b,c): $(\alpha, \beta) = (0.10, 0.10)$ and, as given in Table 2, we here found $(\alpha, \beta) = (1.00, 0.00)$. Large difference found for the α parameter comes from the different value of the mass-to-light ratio estimated in the inner part of this galaxy. In S07b,c we used $M/L_B = 3.9$ which is much higher than the more precisely established value of $M/L_B = 1.2$ calculated in S14 and used in the present work.

b) for the galaxy NGC 5846 the following pair was inferred: $(\alpha, \beta) = (0.30, 0.30)$ (see S07b). In the present work, both α and β parameters were found to be higher, $(\alpha, \beta) = (0.70, 0.60)$ (the value of β is the highest for the sample). Here, the difference comes not so much from the value of the mass-to-light ratio in the innermost part (in S07c the value $M/L_B = 9$ was used) but from the fact that here we used the estimate of the mass-to-light ratio at $5R_e$ and in S07c the lower M/L value at $3.2R_e$ was used ($M/L_B = 20$). The new, updated, estimate at $\sim 3R_e$ is $M/L_B \sim 35$.

[2] For clarity, for the theoretically expected results only the central values of the concentration parameter are presented.

These new, more accurate results, show that more observations of ETGs are needed in order to constrain more firmly the available theoretical models.

Table 2. Best fit values of the slope parameters (α, β) for the galaxies presented in Table 1.

name (1)	α (2)	β (3)	Υ_0 (4)	Υ_1 (5)	$\bar{\chi}^2$ (6)
NGC 1400	0.60 ± 0.20	-0.20 ± 0.20	6.7	12.1	0.04
NGC 1407	1.00 ± 0.05	0.10 ± 0.10	8.0	47.7	0.02
NGC 2768	0.20 ± 0.05	-0.10 ± 0.10	12.8	14.4	0.04
NGC 3115	0.70 ± 0.05	0.10 ± 0.05	13.1	50.9	0.39
NGC 3377	0.40 ± 0.20	-0.10 ± 0.20	6.6	10.5	0.02
NGC 4278	0.70 ± 0.10	-0.20 ± 0.05	14.3	31.0	0.13
NGC 4494	1.00 ± 0.10	0.00 ± 0.05	1.2	5.9	0.001
NGC 5846	0.70 ± 0.05	0.60 ± 0.05	7.1	64.5	0.51

NOTES – Column (1): name of the galaxy. Column (2): Best-fitting value of the α parameter with formal error. Column (3): Best-fitting value of the β parameter with formal error. Column (4): Value of the scaling M/L ratio (corresponds to the value of the M/L ratio at $1R_e$). Column (5): Value of the M/L ratio at $5R_e$. Column (6): Best-fitting value of the reduced $\bar{\chi}^2$ parameter. The values of the M/L ratio are given in the B-band.

Table 3. The estimated virial mass, $M_{\rm vir}$, the concentration parameter for the observational and theoretical case, $c_{\rm obs}$ and $c_{\rm th}$, respectively, of the galaxies in the sample.

name (1)	$M_{\rm vir}$ $[M_\odot]$ (2)	$c_{\rm obs}$ (3)	$c_{\rm th}$ (4)
NGC 1400	$1.05^{+0.59}_{-0.57} \times 10^{12}$	$5.38^{+0.87}_{-1.24}$	15.3
NGC 1407	$1.17^{+0.43}_{-0.42} \times 10^{13}$	$7.53^{+0.82}_{-1.03}$	11.2
NGC 2768	$6.02^{+3.28}_{-3.03} \times 10^{11}$	$6.35^{+0.99}_{-1.32}$	16.5
NGC 3115	$1.39^{+0.50}_{-0.46} \times 10^{12}$	$18.07^{+1.95}_{-2.27}$	14.8
NGC 3377	$2.28^{+1.96}_{-1.82} \times 10^{11}$	$7.03^{+1.61}_{-2.89}$	18.7
NGC 4278	$5.89^{+2.68}_{-2.65} \times 10^{11}$	$17.35^{+2.31}_{-3.14}$	16.5
NGC 4494	$1.29^{+0.90}_{-0.82} \times 10^{12}$	$5.82^{+1.12}_{-1.68}$	14.9
NGC 5846	$6.56^{+3.61}_{-3.55} \times 10^{12}$	$14.99^{+2.36}_{-3.43}$	12.1

Conclusion

We studied the sample of 8 ETGs for which we have estimates of the gradient of their mass-to-light ratio between 1 and 5 effective radii. We used a phenomenological approach to infer the importance of DM in their mass

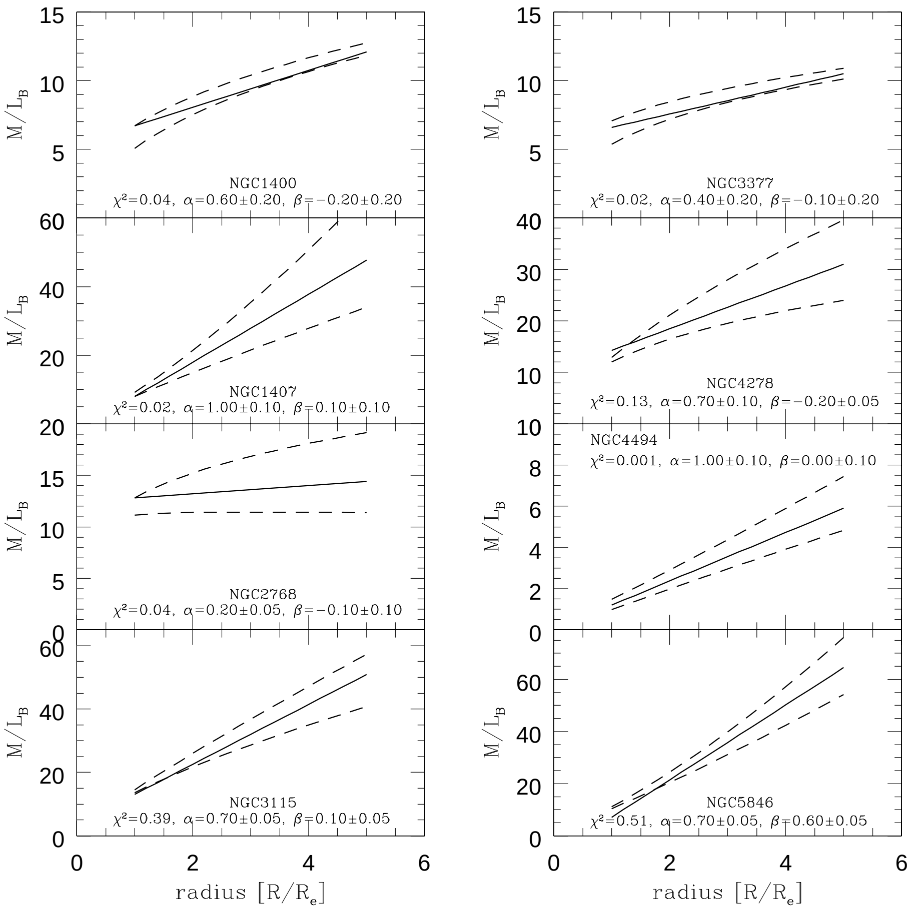

Fig. 1. Mass-to-light ratio profiles of the galaxies in our sample in the B-band. Radius is given in units of effective radius and for individual galaxies can be found in Table 1. Solid line is an "observational" one and two dashed lines indicate upper and lower limits of the modeled mass-to-light ratio (see the text for details). The solid line based on the slope parameters from Table 2 is between the limits: the value of the M/L ratio at $1R_e$ is Υ_0 and the value of the M/L ratio at $5R_e$ is Υ_1 (see Table 2).

content. Using the formula proposed by TCP07 (see equation 1), we calculate the slope parameters α and β and compare their calculated values with the theoretical predictions which come from numerical simulations.

We found that there is no galaxy in our sample for which $(\alpha, \beta) = (0, 0)$, i.e., there is no ETG for which there is no increase in its mass-to-light ratio: for all the galaxies in our sample an increase of the cumulative mass is found and different amounts of DM are required. For all the galaxies in our

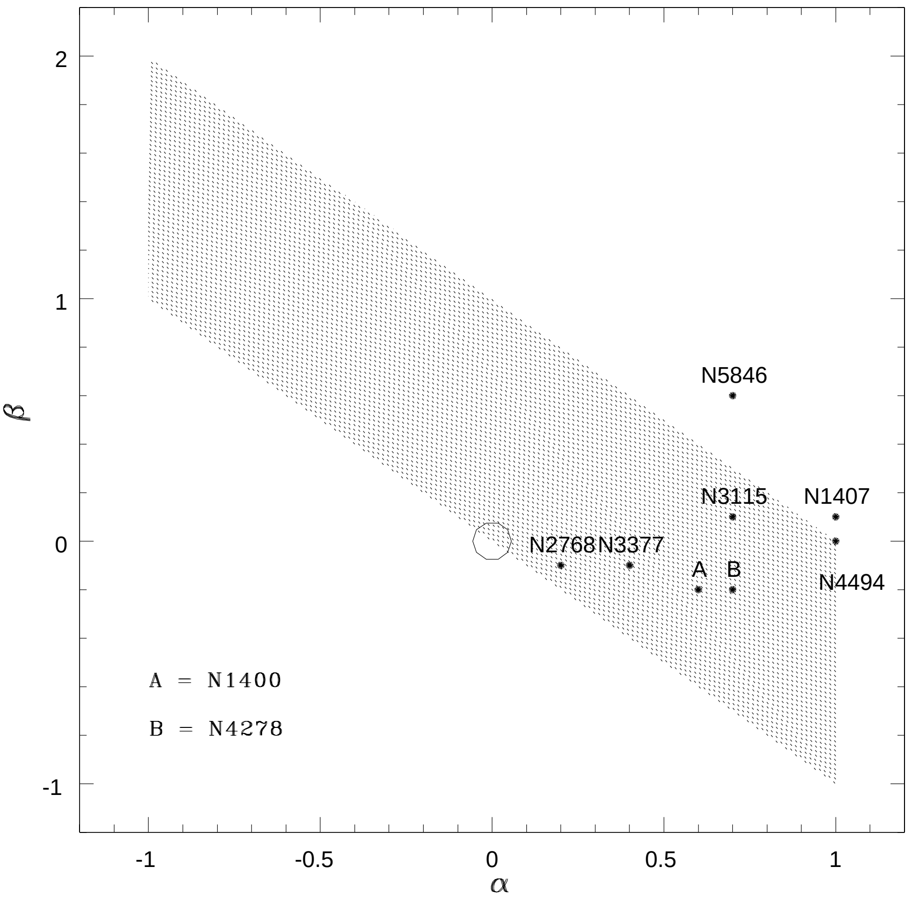

Fig. 2. Calculated values of the slope parameters α and β for the sample of galaxies used in this paper. The hatched region is a zone permitted by theoretical considerations and is based on equation 2, assuming the Hernquist (1990) model of the luminosity density. Open circle stands for $(\alpha, \beta) = (0, 0)$, the case of the constant mass-to-light ratio.

sample we have: $\alpha + \beta > 0$. The galaxies with higher values of $\alpha + \beta$ have also higher values of their virial mass: we found that for galaxies for which $\alpha + \beta > 0.50$, one can expect the virial mass, $M_{\rm vir} > 1.1 \times 10^{12} M_{\odot}$.

We found that for only one galaxy (NGC 5846) the calculated pair $(\alpha, \beta) = (0.70, 0.60)$ is beyond the theoretical boundaries. This is the object with high virial mass and the highest mass-to-light ratio measured at its outermost point, $M/L_B = 64.5$.

We show that two galaxies which are *slow* rotators (NGC 1407 and

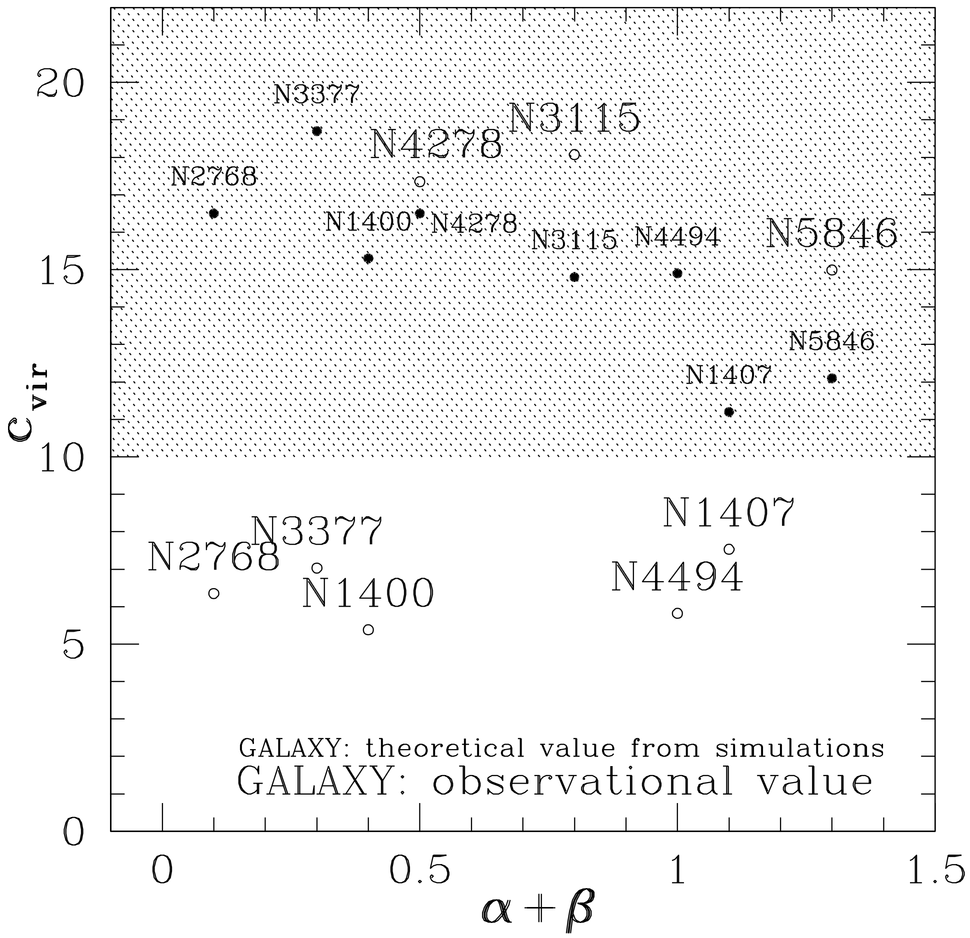

Fig. 3. Values of the sum $\alpha+\beta$ vs. the value of the $c_{\rm vir}$ parameter for the NFW model (see Table 3). The hatched region above $c_{\rm vir}=10$ is based on the work of Wechsler et al. (2002) (see the text for details). The observational values are given in the big characters whereas the theoretical values are plotted in the small characters. Filled circles denote the exact positions of the galaxies based on the theoretical values from simulations and the open circles denote the exact positions of the galaxies based on the observational values.

NGC 5846) have $\alpha+\beta>1$ whereas the remaining 6 galaxies are all *fast* rotators and for these objects $\alpha+\beta\leq 1$.

The comparison of our observationally based results with the theoretical predictions coming from numerical simulations show that while for some objects a reasonable agreement is found, for some other a large discrepancies exist: this is worth investigating in more detail and is left for future work. Here, we found that for galaxies for which $\alpha + \beta < 0.50$, huge discrepancies between the theoretically and observationally inferred values of the concentration parameter are detected.

Our comparison with the previously obtained results (based on NGC 4494 and NGC 5846) confirms that more observational efforts related to ETGs are needed in order to constrain the available theoretical models more accurately.

This work was supported by the Ministry of Education, Science and Technological Development of the Republic of Serbia through the project no. 176021, "Visible and Invisible Matter in Nearby Galaxies: Theory and Observations". This research made use of the NASA/IPAC Extragalactic Database (NED), which is operated by the Jet Propulsion Laboratory, California Institute of Technology, under contract with the National Aeronautics and Space Administration. We acknowledge the usage of the HyperLeda database (`http://leda.univ-lyon1.fr`).
The author thanks Dr. Zorica Cvetković for the encouragement. The author expresses his gratitude to Dr. Tsvetan B. Georgiev for the prompt and useful report and the editorial board for their helpful suggestions.

References

Boriello A., Salucci P., Danese L., 2003, MNRAS, 341, 1109
Bullock J.S., Kolatt T.S., Sigad Y., Somerville R.S., Kravtsov A.V., Klypin A.A., Primack J.R., Dekel A., 2001, ApJ, 321, 559
Hernquist L., 1990, ApJ, 356, 359
Navarro J. F., Frenk C. S., White S.D.M., 1996, ApJ, 462, 563
Navarro J. F., Frenk C. S., White S.D.M., 1997, ApJ, 490, 493
Pota V., Forbes D.A. Romanowsky A.J. et al., 2013, MNRAS, 428, 389
Samurović S., 2007a, Dark Matter in Elliptical Galaxies, *Publications of the Astronomical Observatory of Belgrade*, No. 81.
Samurović S., 2007b, *Serb. Astronom. J.*, 174, 35
Samurović S., 2007c, *Serb. Astronom. J.*, 175, 7
Samurović S., 2014, A&A, 570, A132
Tortora C., Cardone V.F., Piedipalumbo E., 2007, A&A, 463, 105
Wechsler R.H., Bullock J.S., Primack J.R., Kravtsov A.V., Dekel A., 2002, ApJ, 568, 52